NRJ THE NEURORADIOLOGY JOURNAL

VOLUME 27 - No. 4 - AUGUST 2014
CENTAURO S.r.l., BOLOGNA
Bimestrale - Poste Italiane s.p.a. - Sped. in a.p. - D.L. 353/2003 (conv. in L. 27/02/2004 n° 46) art. 1, comma 1, DCB/BO
Euro 30,00

ISSN 1971-4009

Official Journal of:

AINR - Associazione Italiana di Neuroradiologia

and:

The Neuroradiologists of Alpe-Adria
ANRS - Albanian Neuroradiological Society
PANRS - Pan Arab NeuroRadiology Society
Radiological Society of Saudi Arabia, Division of Neuroradiology
Egyptian Society of Neuroradiology
ISNR - Indian Society of Neuroradiology
Indonesian Society of Neuroradiology
Neuroradiology Section of the Radiology Society of Iran
Israeli Society of Neuroradiology
College of Radiology Malaysia
Neuroradiology Section - Pakistan Psychiatry Research Center
Section of Neuroradiology - Polish Radiological Society
The Neuroradiologists of Romania
Section of Neuroradiology of Serbia and Montenegro
SILAN - Sociedad Ibero Latino Americana de Neurorradiologia
Neuroradiology Section of Singapore Radiological Society
Slovenian Society of Neuroradiology
The Neuroradiological Society of Taiwan
TSNR - Turkish Society of Neuroradiology

Semi-Automatic Volumetric Segmentation of the Upper Airways in Patients with Pierre Robin Sequence

SERGIO SALERNO[1], CESARE GAGLIARDO[1], SALVATORE VITABILE[1], CARMELO MILITELLO[2], GIUSEPPE LA TONA[1], MARIO GIUFFRÈ[3], ANTONIO LO CASTO[1], MASSIMO MIDIRI[1]

[1] Department of Biopathology and Medical and Forensic Biotechnologies - Section of Radiological Sciences, University of Palermo; Palermo, Italy
[2] Institute of Molecular Bioimaging and Physiology, National Research Council (IBFM-CNR); Cefalù, Italy
[3] Department of Science for Health Promotion and Mother and Child Care, University of Palermo; Palermo, Italy

Key words: Pierre Robin sequence, multidetector CT, airways segmentation, region growing, 3D rendering, airway model reconstruction

SUMMARY – *Pierre Robin malformation is a rare craniofacial dysmorphism whose pathogenesis is multifactorial. Although there is some agreement in non-invasive treatment in less severe cases, the dispute is still open on cases with severe respiratory impairment. We present a semi-automatic novel diagnostic tool for calculating upper airway volume, in order to eventually address surgery in patients with Pierre Robin Sequence (PRS). Multidetector CT datasets of two patients and two controls were tested to assess the proposed method for ROI segmentation, upper airway volume computation and three-dimensional reconstructions. The experimental results show an irregular pattern and a severely reduced cross-sectional area (CSA) with a mean value of 8.3808 mm² in patients with PRS and a mean CSA value of 33.7692 mm² in controls (a ΔCSA of about -75%). Moreover, the similarity indexes and sensitivity/specificity values obtained showed a good segmentation performance. In particular, mean values of Jaccard and Dice similarity indexes were 91.69% and 94.07%, respectively, while the mean values of specificity and sensitivity were 96.69% and 98.03%, respectively. The proposed tool represents an easy way to perform a quantitative analysis of airway volume and useful 3D reconstructions.*

Introduction

Pierre Robin malformation is an uncommon craniofacial dysmorphism characterized by severe micro or retrognathia, gloss ptosis, respiratory obstruction, and a cleft palate [1]. The condition was first described in 1923 by the French dental surgeon Pierre Robin [2] as a syndrome. However, because of the dynamics of developing clinical events it is currently called PRS. Severe micro or retrognathia leads to abnormal backward displacement of the tongue often resulting in a cleft palate [1], difficulties in breathing and feeding, ear infections and reduced hearing. PRS could also be associated with other severe craniofacial syndromes such as Stickler syndrome (40%) or velo-cardio-facial syndrome (15%) [3]. Genetic testing is highly recommended for these patients because the pathogenesis of this condition can be multifactorial and syndromic in nearly half of the occurrences of PRS [1,4-8].

Breathing impairment is a major problem in patients with PRS [9-11]. The assessment of the impairment is based on clinical parameters (episode of desaturation, spontaneously and during feeding and sleep) and growth of facial structures during the first two years of life [9-12]. Many clinicians suggest treating mild cases with prone positioning using special "sniffing air" beds or other non-invasive respiratory support [13]. In cases of severe respiratory impairment surgery is required [14]. However, there is no widely recommended surgical treatment [14,15]. Four major clinical or surgical options are available: nasopharyngeal airway [16], tongue-lip

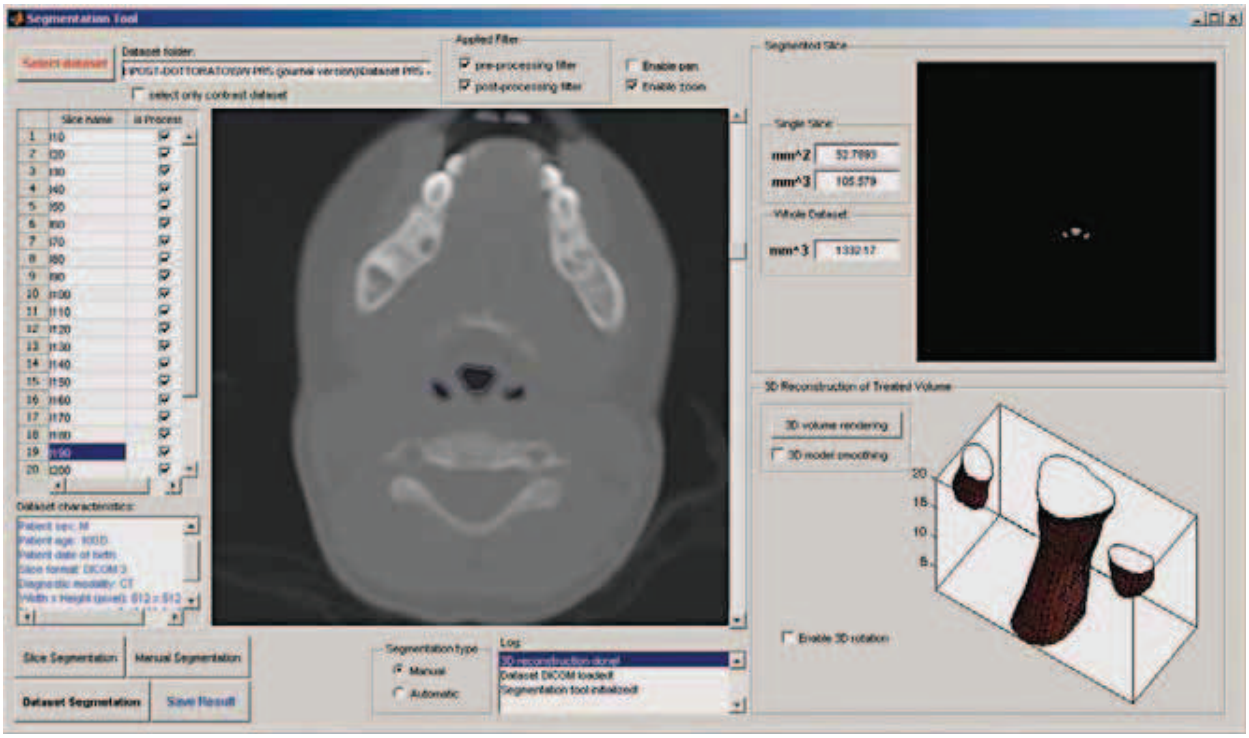

Figure 1 The graphical user interface of the developed tool. Left: the list of the dataset slices and the current-selected slice. Top-right: the segmented ROI. Bottom right: the reconstructed 3D model.

adhesion [17], floor-of-mouth release [18], and distraction osteogenesis [19]. All these procedures have a severe impact on everyday life and significant morbidity [13].

In making a treatment decision a precise assessment of upper airway patency is crucial to avoid spontaneous desaturation or asphyxiation episodes during feeding and sleeping. This study proposes a segmentation tool, ad hoc developed and implemented, to assess more objectively the conductive capacity of the upper airways. The semi-automatic tool is based on an advanced region-growing approach for region of interest (ROI) extraction. In addition, it implements a powerful three-dimensional model for segmented airway reconstruction.

Materials and Method

Two PRS patients (1 male, 1 female, mean age 62 days, mean weight 2465 g) with severe respiratory impairment, and two controls (1 male, 1 female, mean age 47.5 days, mean weight 2440 g) with no craniofacial anomalies but with similar age, sex and weight underwent a craniofacial and neck multidetector CT (MDCT) study. The local ethical committee approved this retrospective study. The two PRS patients were submitted to MDCT examination for a preliminary evaluation of upper airway calibre and to exclude other cranial malformations. MDCT scans were performed with the following parameters: detector configuration 16×0.625 with a collimation of 10 mm and a pitch of 0.562:1 with 120Kv and 100mA, matrix size 512×512 pixels (CTDI vol 22.30 mGy; DLP 204.95 mGy*cm). All patients underwent MDCT mildly sedated in spontaneous breathing. The scan technique for controls was adopted for both brain and maxillofacial bones as the examinations were done for clinical reasons other than patency of the airway (Table 1).

Table 1 Patient characteristics.

Dataset	*Gender*	*Age (days)*	*Weight (g)*
Control 1	Male	60	2710
Control 2	Female	35	2170
PRS 1	Male	84	2500
PRS 2	Female	40	2430

Slices from the hard palate to the laryngeal plane obtained from the MDCT studies were processed using the proposed tool and developed in MATLAB (The MathWorksInc ®) which allows upper airway segmentation, upper airway volume computation and 3D volume reconstruction.

The segmentation algorithm used is based on a dynamic region-growing procedure that exploits the different density of anatomical structures, resulting in a strong brightness contrast between the upper airways and surrounding tissues. The algorithm shows good performances in term of accuracy as demonstrated by the related Jaccard and Dice [20,21] similarity indexes and by sensitivity and specificity values. As shown in Figure 1, the graphical user interface (GUI) developed is intuitive and allows slices of interest to be selected from the MDCT dataset and displays the segmented area of each slice and the overall resulting volume. The possibility to zoom/move the 3D model allows the physician to interact with the GUI and display details on the 3D volume-rendering (3D-VR) model from every point of view.

Interpolation was used to improve the 3D-VR reconstruction results but is obviously dependent on the original slice thickness. In particular, starting from two consecutive slices, interpolation produces a third slice that will be positioned in the middle of two initial slices. The 3D interpolated model has a more natural shape, without the typical saw-tooth trend otherwise obtained.

A dynamic region-growing algorithm was used for airway ROI segmentation. The algorithm starts from a seed-point selected by mouse-clicking the structure of interest. This technique is even better than those based on global or adaptive threshold since it does not require any highlighted area of interest. The region-growing algorithm used allows an easy selection of pixels having brightness affinity with the given seed-point (Figure 2A,B). After the segmentation procedure, an edge-detection algorithm extracts the useful data for the airway volume reconstructions. In Figure 2B the red circle highlights the selected seed-point, whereas the blue contour represents the edge of the segmented ROI.

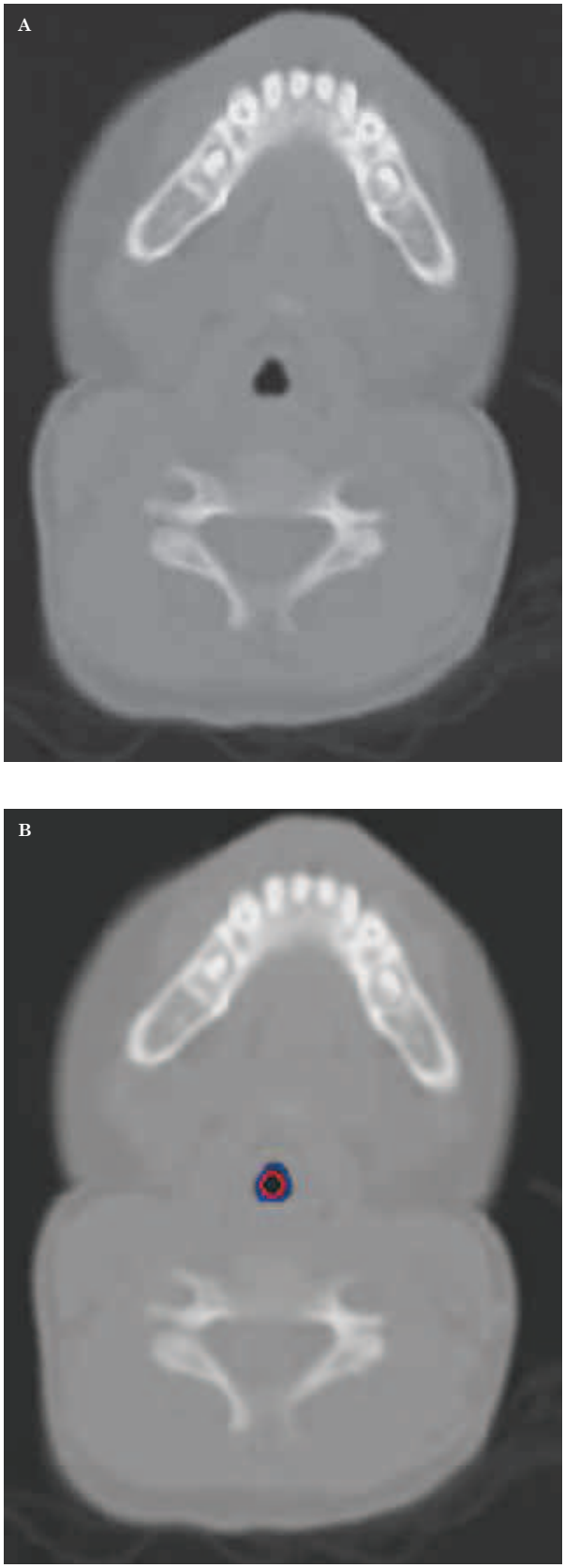

Figure 2 ROI segmentation on a healthy control. A) Original slice. B) The segmented ROI after the region-growing process. The red circle highlights the initial seed-point in the slice. The superimposed blue edge highlights the boundary of the segmented ROI.

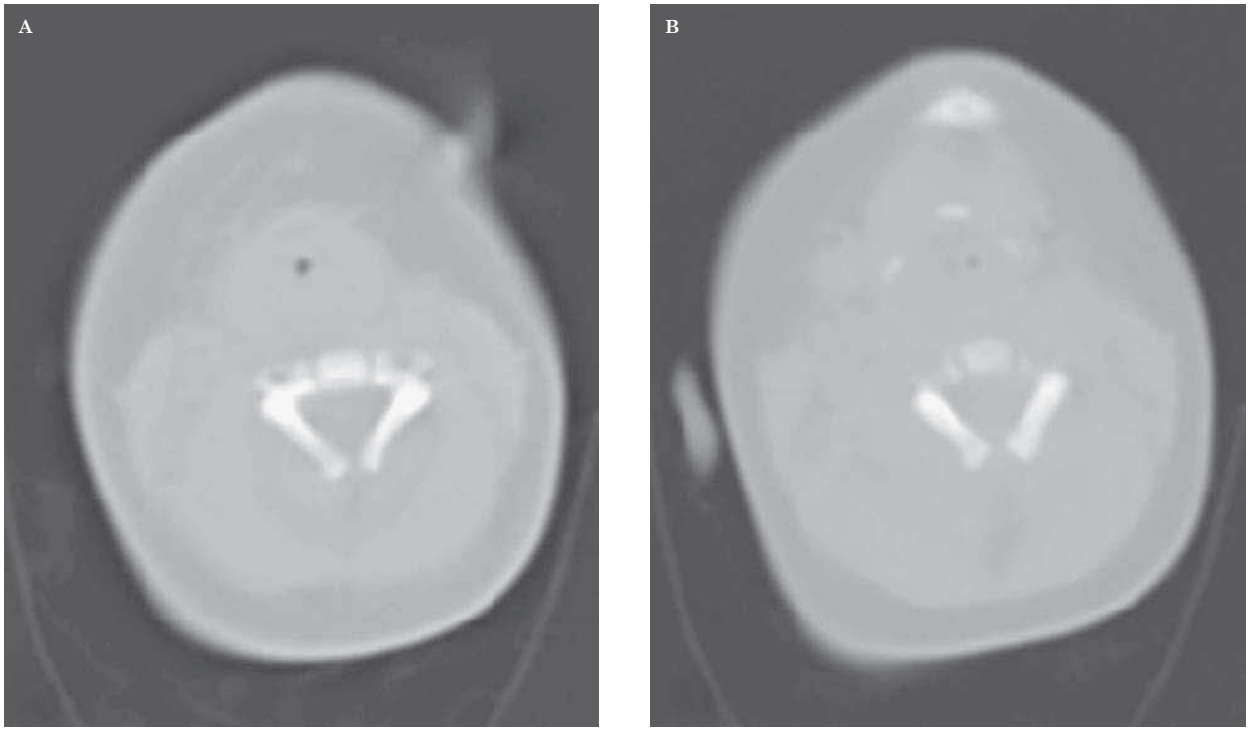

Figure 3 A-C) Three slices from a PRS case dataset. The significantly reduced airway calibre can create problems with the region-growing based segmentation. For this reason, an advanced version of the algorithm has been implemented.

The growing procedure checks if the pixel is within the image, if the pixel has not already been added to the ROI and if the value of the pixel satisfies the threshold condition. If these conditions are met the pixel is then added to the ROI. The value of the threshold used is set using the Otsu algorithm [22]. PRS patients may show severe upper airway stenosis (Figure 3A,B). Considering that the patients we studied are not intubated (to avoid any airway calibre distortion), the airway can be very narrow (Figure 3C). In these cases the region-growing procedure results in an incomplete segmentation and consequently affects the 3D-VR model.

For these reason, an advanced version of the described region-growing algorithm was used. The new algorithm requires the selection of two points in the slices at the level of the stenosis: the first inside the ROI and the second on the surrounding tissues (Figure 4A,B).

ROI segmentation was also used for 3D-VR reconstructions, allowing a panoramic view of the upper airway morphology, providing useful information on the severity of the disease, and aiding surgical planning (Figure 5A: control patient; Figure 5B: PRS patient). The ROI edges extraction process is followed by three main post-processing steps, leading to 3D-VR reconstructions: (i) isosurface extraction from

the dataset; (ii) generation of polygons set for isosurface approximation; (iii) normal surface computation to achieve a blunter surface. To increase the visual quality of the 3D-VR model, an optional filtering step was performed to soften the edges and avoid the "edginess" of the polygon-based surface. Adding some virtual light sources completes the final 3D-VR model.

The proposed segmentation approach evaluation was performed by calculating Jaccard and Dice similarity indexes through equations (1) and (2) [20,21]. Specificity and sensitivity values were calculated through equations (3) and (4). Results obtained with the proposed region-growing approach and the manually segmented ROIs produced by an experienced radiologist, were compared.

$$JaccardIndex(N_M, N_A) = \frac{|N_M \cap N_A|}{|N_M \cap N_A|} \quad (1)$$

$$DiceIndex(N_M, N_A) = \frac{2|N_M \cap N_A|}{|N_M| + |N_A|} \quad (2)$$

$$Sensitivity = \frac{N_{T_P}}{|N_M|} \quad (3)$$

$$Specificity = 1 - \frac{N_{F_P}}{|N_A|} \quad (4)$$

where:
N_M is the segmented area manually selected by the radiologist;
N_A is the automatic segmented area using the proposed approach;
N_{T_P} is the number of true positive voxels;
N_{F_P} is the number of false positive voxels.

Results

An initial graphic assessment of the 3D model obtained highlights some features for a first quantitative analysis. In particular, in PRS patients it is possible to see a high value of the standard deviation (SD) associated with "section irregularities" of the segmented and extracted ROIs (Table 2). Moreover, it is possible to note a lower volume in PRS patients compared to healthy patients.

Table 2 Information on the cross-sectional area (CSA) obtained with the proposed approach. Mean value is computed on the set of processed slices.

Dataset	*mean CSA (mm^2)*	*CSA SD (mm^2)*
Control 1	46.9130	3.2599
Control 2	20.6254	2.5183
PRS 1	8.7340	8.4115
PRS 2	8.0276	5.3400

Table 3 Evaluation of the segmentation results using Jaccard and Dice [18-19] similarity indexes. Mean values are computed on the set of the processed slices.

Dataset	*Jaccard Index (%) (mean value ± SD)*	*Dice Index (%) (mean value ± SD)*
Control 1	92.2677 ± 0.036	95.9424 ± 0.020
Control 2	92.2939 ± 0.028	95.9716 ± 0.015
PRS 1	84.5148 ± 0.344	85.5632 ± 0.348
PRS 2	97.6948 ± 0.034	98.8055 ± 0.018

Table 4 Sensitivity and specificity values of the proposed segmentation approach. Mean values are computed on the set of the processed slices.

Dataset	*Sensitivity (%) (mean value ± SD)*	*Specificity (%) (mean value ± SD)*
Control 1	94.2441 ± 0.050	97.4204 ± 0.015
Control 2	94.8577 ± 0.030	96.9852 ± 0.023
PRS 1	98.6336 ± 0.020	99.1434 ± 0.013
PRS 2	99.0383 ± 0.026	98.5644 ± 0.018

Table 3 shows the mean values of Jaccard and Dice [20,21] indexes and their relative SD with the corresponding sensitivity and specificity values. Table 4 shows sensitivity and specificity ratios.

The data collected from healthy patients revealed a regular pattern with a well appreciable calibre of the laryngeal-pharyngeal tract showing a mean CSA of 33.7692 mm^2. Instead, in PRS patients, the upper airways showed an irregular pattern and a severely reduced CSA with a mean value of 8.3808 mm^2. In one case we found a severe stenosis of the air duct, but in all PRS cases we found a significantly lower mean CSA (about –75%). Also comparing the mean CSA SD of control (2.8891 mm^2) vs PRS (6.8758 mm^2) datasets it was possible to see the irregularity of the airways in PRS patients.

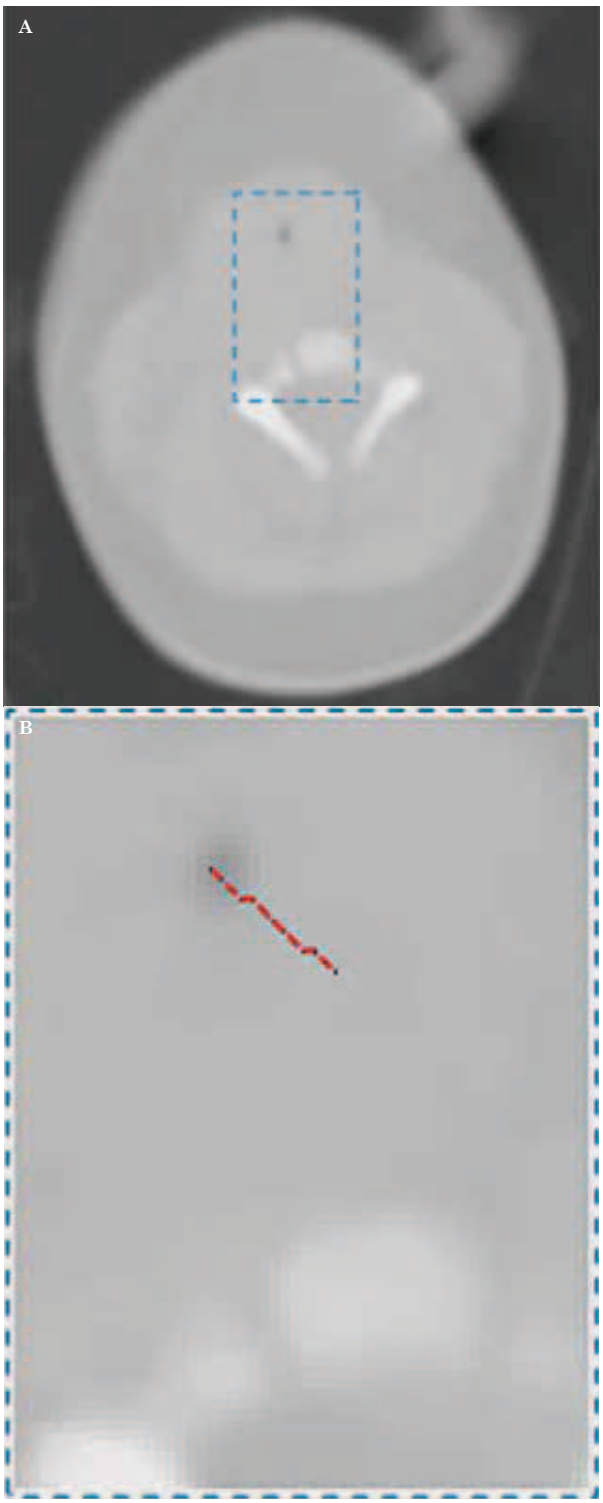

Figure 4 The advanced region-growing algorithm. The algorithm requires the selection of two points in the slices at the stenosis level: the first is inside the ROI, while the second is on the surrounding tissues. A) The original slice with evident stenosis. B) The zoomed detail of airway neighbourhood with the superimposed red straight between the ROI and the surrounding tissue.

Discussion

Upper airway patency is the focus key point for patients with PRS. The risk of spontaneous desaturation or asphyxiation episodes during feeding or sleeping requires continuous monitoring of these young patients.

The similarity indexes (Jaccard and Dice mean indexes are 91.69% and 94.07%, respectively) and specificity and sensitivity ratios (mean values are 96.69% and 98.03%, respectively), used to evaluate the region-growing based approach, showed a good segmentation performance. Even if consensus exists for treating mild cases with prone positioning alone or for treating with tracheostomy cases with severe subglottic obstructions, there is still an ongoing controversy on whether and how many of the remaining mild cases will have a catch-up growth of the underdeveloped mandible. As brilliantly summarized by Mackay in his analysis of controversies in the diagnosis and management of PRS [12], approximately 70% of all patients with PRS will be successfully managed by prone positioning alone, while in rare cases tracheostomy will be necessary (10%). Major controversy exists on what to do in the remaining 20% of patients with PRS. In addition, we cannot forget the morbidity and mortality rate of tracheostomy in infants [13-15].

The possibility to measure upper airway volume to choose patients eligible for surgery could be decisive for patients' outcome. The preliminary results seem to meet the requirements for this kind of evaluation and the developed segmentation algorithm may be integrated in a medical decision support system. If ad-hoc developed and implemented to segments of PRS patient airways, our tool has some limits. First, our method depends on breathing so we decided to acquire all examinations in mildly sedated patients without a respiratory synchronized protocol, avoiding general anaesthesia and/or tracheal intubation to reduce modifications of airway calibre. However cases with thin parts membranecea of the trachea acquired in full inspiration may need an additional manual editing reconstruction to avoid false overestimation of the narrow sections. The second limitation of our study is the sample population. Even if our population was small, the overall low incidence of PRS cases should also be considered and, among these, those who require surgical treatment (30% of all) [2,8,15].

Considering these limits, our segmentation tool represents a very easy way to make

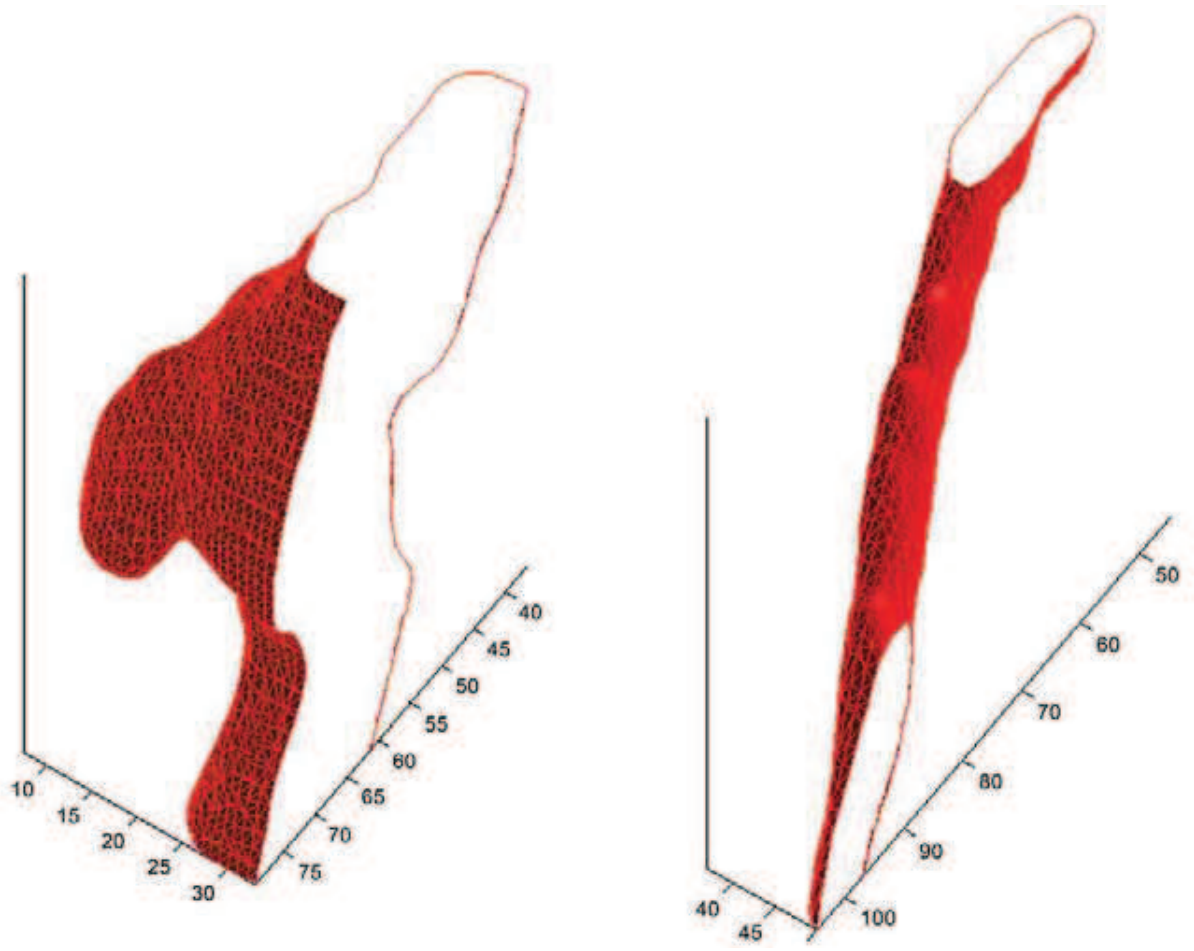

A B

Figure 5 Examples of 2 3D-VR reconstructions. A) Sectioned view of the 3D airway model of a control dataset: the obtained reconstruction shows a regular airway pattern with appreciable and regular cross-section areas. B) Sectioned view of the 3D airway model of a pathological dataset: the obtained reconstruction shows a very irregular airway pattern with a reduced cross-section area and no axial symmetry in structures.

a quantitative analysis of airway volume. The tool also provides three-dimensional reconstructions, which represent the best intuitive images for surgeons, who usually prefer a panoramic view of the structure they are going to treat. The evolutions of this heterogeneous but rare disease remain controversial together with the treatment options. Today case-by-case analysis and a multidisciplinary evaluation and management should probably be considered the optimal option to achieve the best outcome for each single patient. In an attempt to contribute to this controversial aspect of the syndrome, we believe that the algorithm proposed could be helpful in the discrimination of severe respiratory impairment in PRS cases.

References

1 Cohen MM Jr. Robin sequences and complexes: causal heterogeneity and pathogenetic/phenotypic variability. Am J Med Genet. 1999; 84 (4): 311-315.doi: 10.1002/(SICI)1096-8628(19990604)84:4<311::AID-AJMG1>3.0.CO;2-9.
2 Robin P. La chute de la base de la langue considérée comme une nouvelle cause de gêne dans la respiration nasopharyngienne. Bull Acad Med (Paris). 1923; 89: 37-41.
3 Evans AK, Rahbar R, Rogers GF, et al. Robin sequence: a retrospective review of 115 patients. Int J Pediatr Otorhinolaringol. 2006; 70 (6): 973-980. doi: 10.1016/j.ijporl.2005.10.016.

4 Carroll DB, Peterson RA, Worton EW, et al. Hereditary factors in the Pierre Robin syndrome. Br J Plast Surg. 1971; 24 (1): 43-47. doi: 10.1016/S0007-1226(71)80008-5.
5 Schreiner RL, McAlister WH, Marshall RE, et al. "Stickler syndrome in a pedigree of Pierre Robin syndrome. Am J Dis Child. 1973; 126 (1): 86-90.
6 Cohen MM Jr. "Dysmorphology, syndromology and genetics". In: McCarthy J, ed. Plastic Surgery. New York: Saunders. 1988. 69-111.
7 Jakobsen LP, Knudsen MA, Lespinasse J, et al. The genetic basis of the Pierre Robin Sequence. Cleft Palate Craniofac J. 2006; 43 (2): 155-159. doi: 10.1597/05-008.1.
8 Abadie V. Isolated Pierre Robin syndrome. Orphanet encyclopedia. 2006. http://www.orpha.net/consor/cgi-bin/OC_Exp.php? lng=en&Expert=718.
9 Takagi Y, McCalla JL, Bosma JF. Prone feeding of infants with the Pierre Robin syndrome. Cleft Palate J. 1966; 3: 232-239.
10 Pielou WD. Non-surgical management of Pierre Robin syndrome. Arch Dis Child. 1967; 42 (221): 20-23. doi: 10.1136/adc.42.221.20
11 Leboulanger N, Picard A, Soupre V, et al. Physiologic and clinical benefits of noninvasive ventilation in infants with Pierre Robin sequence. Pediatrics. 2010; 126: e105610- e105663. doi: 10.1542/peds.2010-0856.
12 Mackay DR. Controversies in the diagnosis and management of the Robin sequence. J Craniofac Surg. 2011; 22 (2): 415-420. doi: 10.1097/SCS.0b013e3182074799.
13 Lidsky ME, Lander TA, Sidman JD. Resolving feeding difficulties with early airway intervention in Pierre Robin Sequence. Laryngoscope. 2008; 118 (1): 120-123. doi: 10.1097/MLG.0b013e31815667f3.
14 Scott AR, Tisebar RJ, Sidman JD. Pierre Robin Sequence evaluation, management, indication for surgery and pitfalls. Otolaryngol Clin N Am. 2012; 45 (3): 695-710, ix. doi: 10.1016/j.otc.2012.03.007.
15 Heaf DP, Helms PJ, Dinwiddie R, et al. Nasopharyngeal airways in Pierre Robin syndrome. J Pediatr. 1982; 100 (5): 698-703. doi: 10.1016/S0022-3476(82)80567-2.
16 Bijnen CL, Don Griot PJ, Mulder WJ, et al. Tongue-lip adhesion in the treatment of Pierre Robin sequence. J Craniofac Surg. 2009; 20 (2): 315-320. doi: 10.1097/SCS.0b013e31819ba5ce.
17 Caouette-Laberge L, Plamondon C, Larocque Y. Subperiosteal release of the floor of the mouth in Pierre Robin sequence: experience with 12 cases. Cleft Palate Craniofac J. 1996; 33 (6): 468-472. doi: 10.1597/1545-1569(1996)033<0468:SROTFO>2.3.CO;2.
18 Dauria D, Marsh JL. Mandibular distraction osteogenesis for Pierre Robin sequence: what percentage of neonates need it? J Craniofac Surg. 2008; 19 (5): 1237-1243. doi: 10.1097/SCS.0b013e3181843293.
19 Jaccard P. Distribution de la florine alpine dans la Bassin de Dranseset dans quellques regions voisines. Bulletin de la Societe Vaudoise des Sciences Naturelles. 1901. Vol. 37, pp. 241-272.
20 Dice LR. Measures of the amount of ecologic association between species. Ecology. 1945; 26, 297-302. doi: 10.2307/1932409.
21 Otsu N. A threshold selection method from gray-level histograms. IEEE Transactions on Systems, Manand Cybernetics. 1979. Vol. 9, No. 1, pp. 62-66. doi: 10.1109/TSMC.1979.4310076.

Sergio Salerno, MD
Via del Vespro, 127
90177 - Palermo (Italy)
Mobile: +39 091 655 23 15
E-mail: sergio.salerno@unipa.it